Comput Geosci (2007) 11:261–274
DOI 10.1007/s10596-007-9050-1

ORIGINAL PAPER

Dynamic capillary effects in heterogeneous porous media

Rainer Helmig · Alexander Weiss · Barbara I. Wohlmuth

Received: 12 January 2007 / Accepted: 13 April 2007 / Published online: 10 July 2007

Abstract In standard multi-phase flow models on porous media, a capillary pressure saturation relationship developed under static conditions is assumed. Recent experiments have shown that this static relationship cannot explain dynamic effects as seen for example in outflow experiments. In this paper, we use a static capillary pressure model and a dynamic capillary pressure model based on the concept of Hassanizadeh and Gray and examine the behavior with respect to material interfaces. We introduce a new numerical scheme for the one-dimensional case using a Lagrange multiplier approach and develop a suitable interface condition. The behavior at the interface is discussed and verified by various numerical simulations.

Keywords Heterogeneous porous media · Dynamic capillary effect · Capillary pressure

R. Helmig
IWS, Department of Hydromechanics and Modeling of Hydrosystems, Universität Stuttgart, Pfaffenwaldring 61, 70529 Stuttgart, Germany
e-mail: helmig@iws.uni-stuttgart.de

A. Weiss (✉) · B. I. Wohlmuth
Institute of Applied Analysis and Numerical Simulations (IANS), Universität Stuttgart, Pfaffenwaldring 57, 70529 Stuttgart, Germany
e-mail: weiss@ians.uni-stuttgart.de

B. I. Wohlmuth
e-mail: wohlmuth@ians.uni-stuttgart.de

1 Motivation

Flow processes in porous media involving two immiscible fluids need to be understood and predicted when dealing with subsurface hydrosystems or industrial applications. For example, in the unsaturated zone, the spatial distribution of the water and air phase as well as their fluxes serve as a basis for modeling transport of contaminants such as pesticides or heavy metals (e.g., [1]). As examples for industrial applications in two-phase flow, the movement of fluids through a filter or the infiltration of ink into paper (see [16]) can be considered. The physical–mathematical model underlying simulations of two-phase flow on the Darcy scale usually requires a constitutive relationship between (wetting phase) saturation S_w and capillary pressure p_c, the $p_c(S_w)$ relationship.

Traditionally, one assumes that this relationship is determined under quasi-static or steady-state conditions but can be applied to any transient flow processes fulfilling the Reynolds number criterion. However, recently some works have questioned this assumption (see, e.g., [17]). These authors were able to improve simulation results by applying a model that accounts for a rate dependence in the $p_c(S_w)$ function. One possibility to obtain this new capillary pressure function is adding a dynamic term, the static capillary pressure relationship (see, e.g., [7–10]).

Although several works recently have analyzed rate-dependent $p_c(S_w)$ relationships or have tried to determine a pertaining additional parameter, the importance of including a rate dependence in the capillary pressure relationship in simulations still needs to be identified. From the simulation point of view, it is very important

to integrate the dynamic $p_c(S_w)$ function into the discretization scheme.

One of the other current challenging questions in the modeling of two-phase flow processes is the approximation of the material interfaces. At these interfaces, the use of a consistent model on the macroscale is mandatory to correctly describe the processes (see [4, 12, 18]). The physical and mathematical complexity of the problem formulation crucially affects the requirements on the associated numerical simulation. Moreover, the heterogeneous material leads to a possibly discontinuous solution at material interfaces. This should be taken into account in the discretization.

In this paper, we present a new discretization scheme for the simulation of dynamic capillary effects in a heterogeneous porous media. A special focus is put on the analysis of the behavior at material interfaces. Therefore, a suitable interface condition based on a hybrid coupling is derived and included into the numerical scheme.

The other parts of the paper are organized as follows. In Section 2, the physical model of two-phase flow is derived; in Section 3, the time and space discretization is presented. The behavior of the saturation at interfaces from a physical view is discussed in Section 4. In Section 5, the numerical results are presented. Finally, in Section 6, we summarize our new approach and give an outlook to further applications.

2 Physical–mathematical model

In this section, we derive the mathematical model describing two-phase flow in a heterogeneous porous media. For a more detailed and more general derivation, we refer to [11].

We consider an incompressible one-dimensional two-phase flow process in heterogeneous porous media. For simplicity, we assume no source/sink term and no gravity influence, which coincides with the case of a horizontal flow without outer influences. In our model of two-phase flow in porous media, we have a wetting phase ($\alpha = w$) and a non-wetting phase ($\alpha = n$). The mass balance of each phase is described by

$$\phi \frac{dS_\alpha}{dt} + \frac{dv_\alpha}{dx} = 0, \quad \alpha \in \{w, n\}, \quad x \in \Omega, \tag{1}$$

where v_α is the Darcy velocity (or Darcy flux) given by the extended Darcy's law,

$$v_\alpha = -\left(\lambda_\alpha K \frac{dp_\alpha}{dx}\right).$$

In this paper, S_α describes the saturation; p_α, the pressure of the phase α; ϕ and K, the porosity and permeability of the soil matrix, respectively; and the mobility λ_α is defined by $\lambda_\alpha := \frac{k_{r\alpha}}{\mu_\alpha}$, where $k_{r\alpha}$ is the relative permeability function and μ_α the viscosity of each phase. The computational domain $\Omega := \mathbb{R}$ is split into two subdomains, the left subdomain Ω_l and the right subdomain Ω_r. The point of the interface is denoted by x_I. We assume, that on each subdomain, ϕ and K are constant.

To close the system, we need two additional supplementary equations. The first is the saturation balance,

$$\sum_{\alpha=w,n} S_\alpha = 1,$$

and the second describes the relation between the pressures,

$$p_c = p_n - p_w,$$

where p_c is a given capillary pressure–saturation function. In this paper, we use the dynamic capillary pressure–saturation model introduced by Hassanizadeh and Gray [8],

$$\begin{aligned} p_{c,l} &= p_{c,l}^{\text{stat}}(S_w) - \tau_l \frac{dS_w}{dt} \quad \text{on } \Omega_l, \\ p_{c,r} &= p_{c,r}^{\text{stat}}(S_w) - \tau_r \frac{dS_w}{dt} \quad \text{on } \Omega_r, \end{aligned} \tag{2}$$

where p_c^{stat} describes the static capillary pressure function and $\tau \geq 0$ is the dynamic factor. In contrast to standard capillary pressure models, the capillary pressure is not only a function of the saturation S_w but also of its time-derivative $\frac{dS_w}{dt}$. The left picture in Fig. 2 shows the two different static capillary pressure functions for the left and right part of the domain (see Fig. 1). The right picture of Fig. 2 depicts the dynamic capillary pressure relationship depending on S_w and $\frac{dS_w}{dt}$ for the left subdomain. On each subdomain, we assume $p_c^{\text{stat}} : [0, 1] \to [0, \infty)$ to fulfill the following conditions:

- p_c^{stat} is continuously differentiable on $(0, 1)$.
- p_c^{stat} is strictly monotonous decreasing
- $p_c^{\text{stat}}(S_w = 1.0) = 0$

Moreover, we assume that τ is constant and nonnegative on each subdomain.

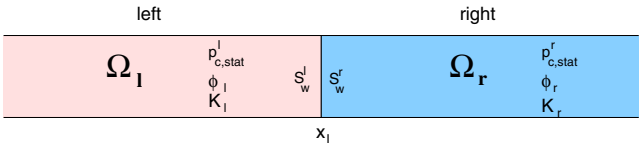

Fig. 1 Material parameters and interface

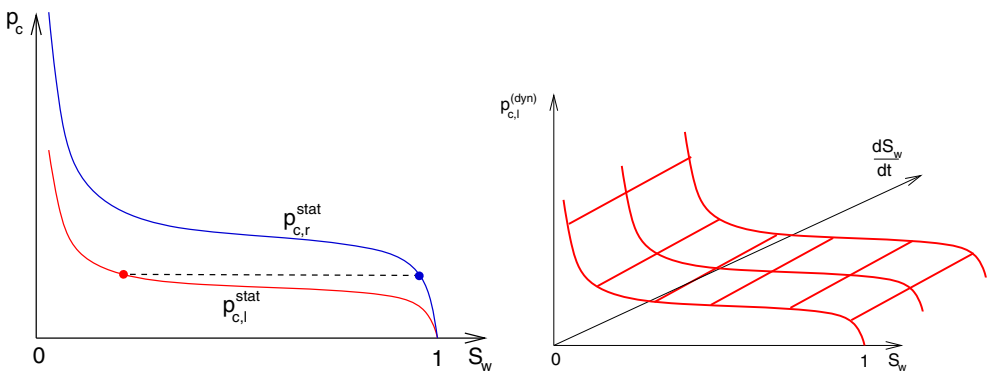

Fig. 2 Static (both domains) and dynamic (only left domain) capillary pressure relationships

We use a fractional flow formulation to get a decoupled set of equations equivalent to the two-phase system (1). For the total velocity defined by $v_t := v_w + v_n$, we get the pressure equation,

$$\frac{dv_t}{dx} = 0,$$

and for S_w, the saturation equation,

$$\phi \frac{dS_w}{dt} + \frac{d}{dx}\left(f_w(S_w)v_t + \bar{\lambda}(S_w)K\frac{dp_c}{dx}\right) = 0,$$

where the fractional flow function f_w is defined by $f_w := \frac{\lambda_w}{\lambda_n+\lambda_w}$ and $\bar{\lambda}$ by $\bar{\lambda} := \frac{\lambda_n\lambda_w}{\lambda_n+\lambda_w}$. The pressure equation implies a constant total velocity. In the sequel, we assume that $v_t > 0$, which corresponds to a flow from the left to the right subdomain. Using the dynamic capillary pressure (2), the saturation equation results in a third order evolution equation for the wetting saturation S_w. To simplify the notation, we denote S_w by s and get

$$\phi \frac{ds}{dt} + \frac{d}{dx}\left(f_w(s)v_t + \bar{\lambda}(s)K\frac{d}{dx}\left(p_c^{\text{stat}}(s) - \tau\frac{ds}{d}\right)\right) = 0,$$

or

$$\phi \frac{ds}{dt} + \frac{d}{dx}\left(f_w(s)v_t + \bar{\lambda}(s)K\left(\frac{dp_c^{\text{stat}}}{ds}(s)\frac{ds}{dx} - \tau\frac{d^2s}{dxdt}\right)\right) = 0. \tag{3}$$

In this formulation, the different parts of the flux term can be easily characterized. The first order term $f_w(s)v_t$ and the third order term $-\bar{\lambda}(s)K\tau\frac{d^2s}{dxdt}$ are convective terms, while the second order term $\bar{\lambda}(s)K\frac{dp_c^{\text{stat}}}{ds}\frac{ds}{dx}$ plays the role of a diffusion term. We will use (3) later to define a suitable time and space discretization.

2.1 Material interfaces

To specify the behavior of the phases at the interface, special interface conditions are needed. For a physical consistent model, we use the continuity of the Darcy flux v_α and the pressure p_α, which directly implies the continuity of the capillary pressure p_c at the material interface.

The continuity of v_α can be obtained by assuming that the time derivative $\frac{ds}{dt}$ of the saturation is bounded and by integrating (1) in a small neighborhood of the interface. The continuity of the capillary pressure at the interface is derived using a regularization technique, see [19].

Let us denote by v_w^l, v_w^r the flux of the wetting phase through the interface on the left and right side of the interface, i.e., $v_w^l = \lim_{x\to x_I^-} v_w(x)$, $v_w^r = \lim_{x\to x_I^+} v_w(x)$. Then the continuity of the flux reads

$$v_w^l = v_w^r$$

In the saturation equation, the flux of the wetting phase is given in terms of the saturation, see (3). Therefore, to fulfill this continuity condition, we introduce the flux through the interface as a new unknown, $v_I = v_w^l = v_w^r$ and obtain

$$v_w^l(s) = v_I = v_w^r(s) \tag{4}$$

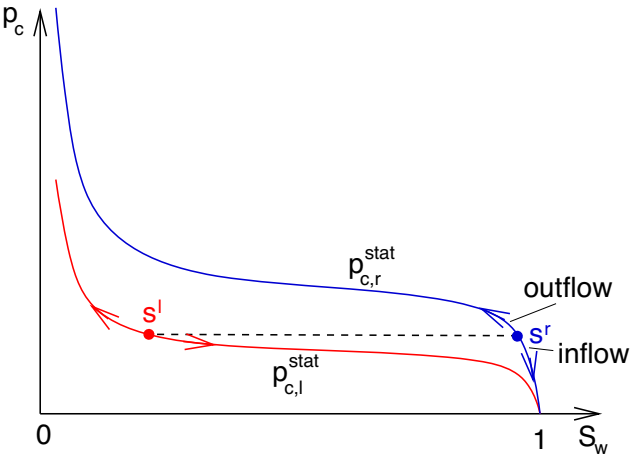

Fig. 3 Relationship of saturations at the interface for static capillary pressure

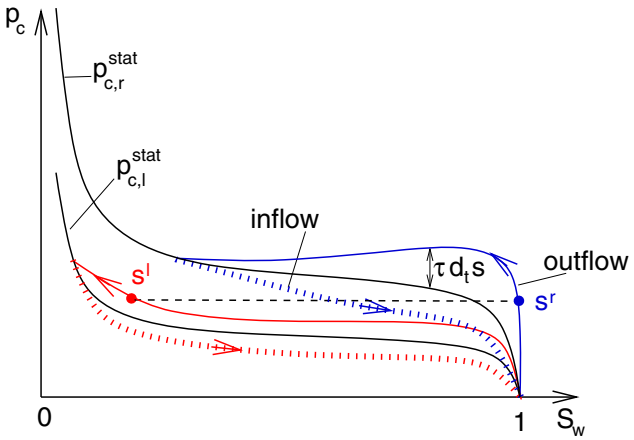

Fig. 4 Relationship of saturations at the interface for dynamic capillary pressure. *Solid* outflow case, *dotted* inflow case

We note that the continuity of the capillary pressure yields no information about the continuity of the saturation; more precisely, it implies in general a discontinuity of the saturation. However, the relationship between the saturations can be specified by using this continuity of pressures,

$$p_c^l = p_n^l - p_w^l = p_n^r - p_w^r = p_c^r.$$

Denoting by s^l, s^r the saturation on the left and right side of the interface, i.e., $s^l = \lim_{x \to x_I^-} s(x)$, $s^r = \lim_{x \to x_I^+} s(x)$, the continuity of the capillary pressure for our dynamic capillary pressure relationship (2) then reads (compare also [2])

$$p_{c,l}^{\mathrm{stat}}(s^l) - \tau_l \frac{ds^l}{dt} = p_{c,r}^{\mathrm{stat}}(s^r) - \tau_r \frac{ds^r}{dt}. \tag{5}$$

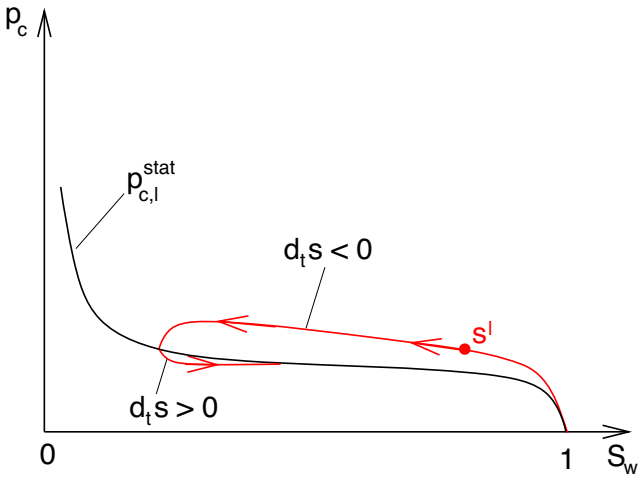

Fig. 5 Saturation and capillary pressure for non-monotonous wave profile

For a static capillary pressure relationship, this implies a discontinuity of the saturation that can be easily specified by the properties of p_c^{stat}, see Fig. 2. As strictly decreasing function, $p_{c,l}^{\mathrm{stat}}$ is invertible, and thus, the saturations are related by $s^l = \left(p_{c,l}^{\mathrm{stat}}\right)^{-1}\left(p_{c,r}^{\mathrm{stat}}(s^r)\right)$. For the dynamic capillary pressure ($\tau > 0$), the situation is more involved. In this paper, the capillary pressure depends on both s and $\frac{ds}{dt}$. As a result, the relationship between the saturations at both sides of the interface is given in terms of an ordinary differential equation. In Section 4, we describe a suitable discretization for this ordinary differential equation.

2.2 Initial conditions and behavior at ∞

As (3) describes a (possibly hyperbolic degenerated) parabolic system, initial and boundary conditions have to be specified. As boundary conditions, we use

$$\lim_{x \to -\infty} s(x) = s^{-\infty}, \quad \lim_{x \to \infty} s(x) = s^{\infty}, \tag{6}$$

with given constant values $s^{-\infty}$ and s^{∞}. As initial condition, we assume that $s(x, 0)$ is smooth on Ω_k for $k = l, r$ and fulfills the boundary conditions (6) as well as a static interface-condition,

$$p_{c,l}^{\mathrm{stat}}(s^l) = p_{c,r}^{\mathrm{stat}}(s^r). \tag{7}$$

3 Discussion of the behavior

In this section, we discuss the solution from a physical point of view. We first recall some results about the behavior in the homogeneous case and then discuss the setting with a material interface.

In the homogeneous case, the evolution of two-phase flow can be determined by considering waves propagating through the homogeneous medium. Therefore, a crucial question is the existence of traveling waves, i.e., waves with a constant wave profile. In the case $\tau = 0$, it is well known that traveling waves have a monotonous profile [19, 20]. In the dynamic case, the existence and behavior of traveling wave solutions was studied in a recent paper ([21], see also [3]). In this

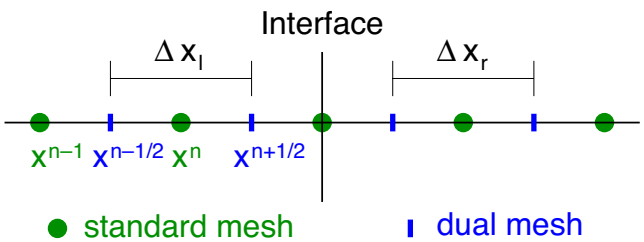

Fig. 6 Standard and dual mesh

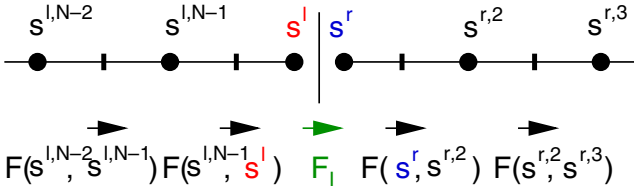

Fig. 7 Discretization of the interface condition

paper, for a value of τ larger then a certain critical value, non-monotonous wave profiles can be observed. This non-monotonous solutions have to be taken into account when discussing the behavior at material interfaces. Moreover, for some parameter settings, one can show that traveling wave solutions do not exist, and we have to consider different types of solution profiles (see, e.g., [13]).

We recall that, in the case of traveling waves, the change of the saturation in time can be derived from the spatial distribution of the saturation. Hence, we assume that we are in a setting where traveling wave solutions – monotonous or non-monotonous – exist, and thus, the information about the time evolution of the saturation is known. For problem settings where no traveling wave solution exists, the behavior at the interface can be derived in a similar way.

We now discuss the solution profile at material interfaces. As the material interface is fixed in space, global traveling wave solutions cannot occur, but at the right side of the interface; that is, Ω_r, we can get a traveling wave solution. Therefore, in our discussion, we assume a behavior of the saturation in time that is generated by a traveling wave solution. We consider inflow processes; that is, the wetting phase displaces the non-wetting phase, and outflow processes, where the wetting phase is displaced by the non-wetting phase.

3.1 Static capillary-pressure

We start with the discussion of the static capillary-pressure relationship, i.e., $\tau = 0$, and recall the basic results, which are given in, e.g., [11]. We recall that traveling waves have a monotonous wave profile, which means that, during an inflow or outflow process, the saturation at each point is a monotonous increasing or decreasing function. At the interface, the continuity of the capillary pressure has to be fulfilled and, hence, we get a discontinuity of the saturation.

First, we consider the outflow process. In the beginning, the non-wetting saturation at both sides of the interface is zero and, hence, the capillary pressure is zero on both sides, too. Then, the saturation increases in a monotonous way. On the saturation–capillary pressure graph, the evolution of the saturation on both sides can be determined by following the graphs of the two functions. The saturations are related to each other by the continuity of the capillary pressure, see Fig. 3. The saturation of the right side s^r then converges to $s^{-\infty}$, which is the time-asymptotic limit. Consequently, the saturation on the left side s^l converges to the saturation that is given by the continuity of the capillary pressure, $\left(p_{c,l}^{\text{stat}}\right)^{-1}\left(p_{c,r}^{\text{stat}}(s^{-\infty})\right)$.

For an inflow process, we assume to start with an equilibrium system (see Section 2.2); therefore, the continuity of the capillary pressure has to be satisfied for the initial conditions. Then, the saturations at both sides increases. Again, the relationship between the saturation of both sides is given by the continuity of the capillary pressure, see Fig. 3. In this manner, the inflow and outflow processes behave the same way at the interface and can be seen as invertible processes.

3.2 Dynamic capillary-pressure – monotonous wave profile

In the case of dynamic capillary pressure, the term $\tau \frac{ds}{dt}$ changes the capillary pressure behavior and thus the behavior of the saturations at the interface. For a

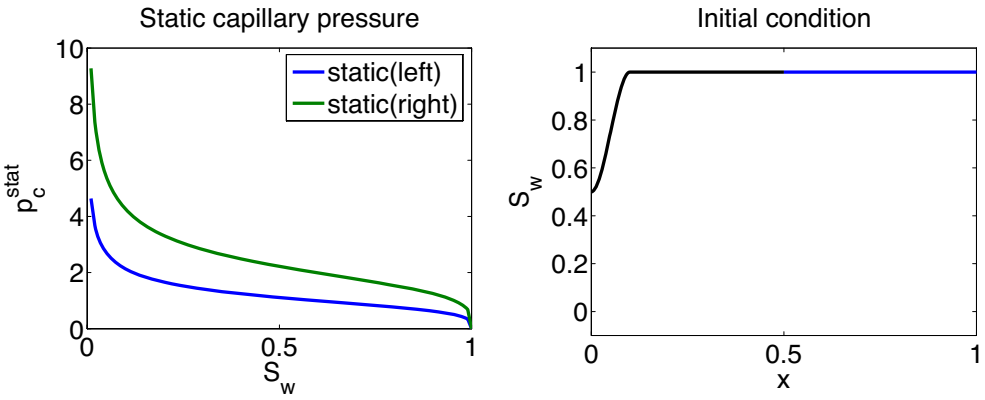

Fig. 8 Static capillary pressure and initial condition for outflow problem

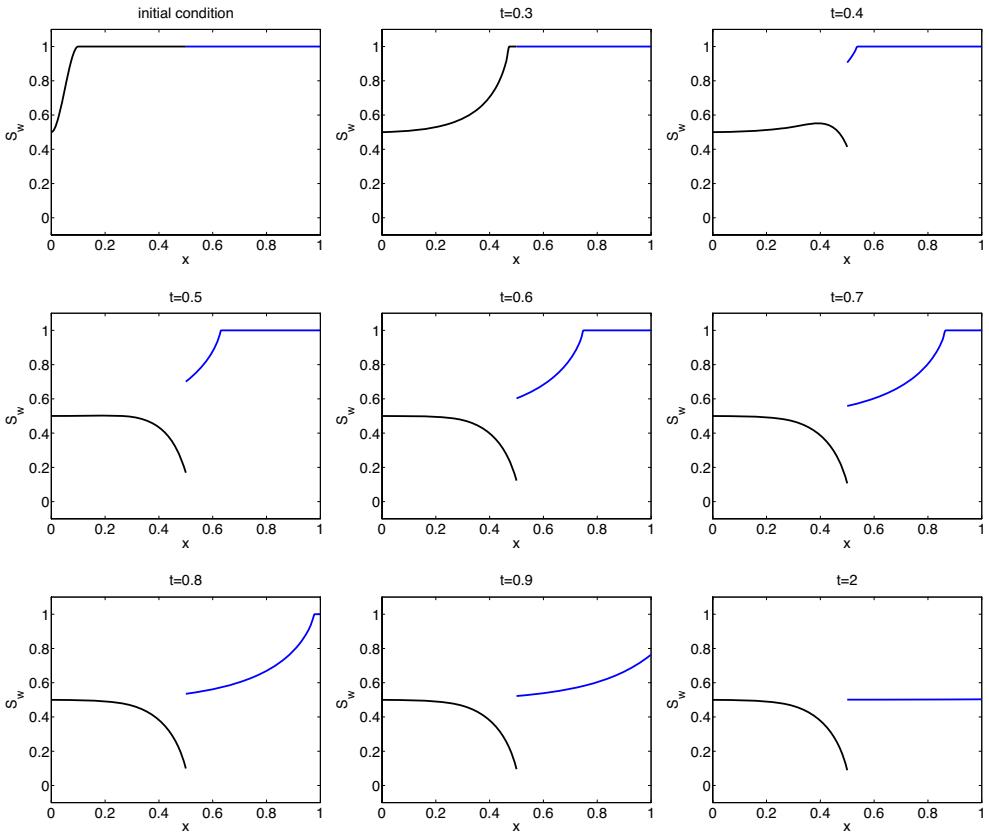

Fig. 9 $\tau_l = \tau_r = 0$, solution at different timesteps

monotonous wave profile, the time-derivative $\frac{ds}{dt}$ does not change the sign and so does the term $\tau\frac{ds}{dt}$. As a result, the static capillary pressure is enlarged for outflow processes and decreased for inflow processes, see Fig. 4. As the saturation is a monotonous function with respect to time, for a given infiltration process, a unique capillary pressure can be assigned to each value of the saturation and for both sides of the interface. However, because of the added dynamic term, it cannot be guaranteed any longer that a unique saturation can be assigned to a given capillary pressure. This is also drafted in Fig. 4. The saturations of both sides are again related by the continuity of the capillary pressure. We note that, in the case of a dynamic capillary pressure, the behavior of an outflow process is completely different to the behavior of an inflow process. For outflow, the dynamic term $\tau\frac{ds}{dt} \geq 0$ increases the static capillary pressure, whereas for inflow processes, the

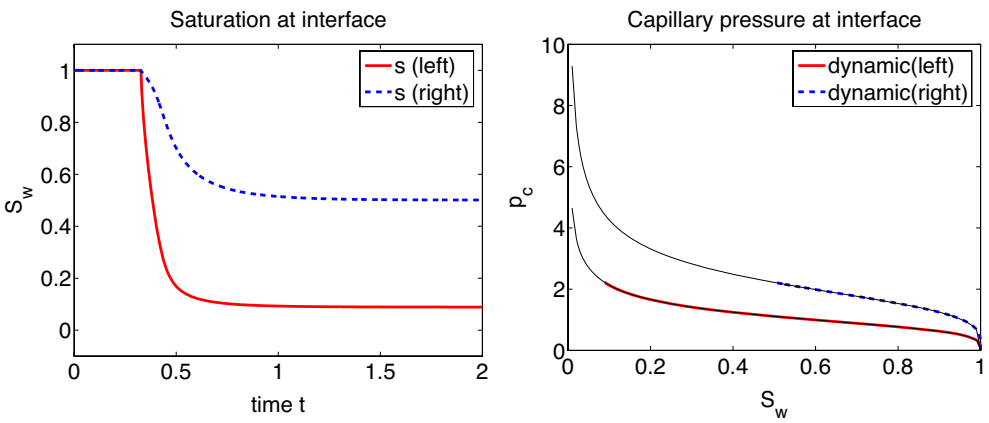

Fig. 10 $\tau_l = \tau_r = 0$. *Left*: behavior of the saturation at the interface, *right* static capillary pressure

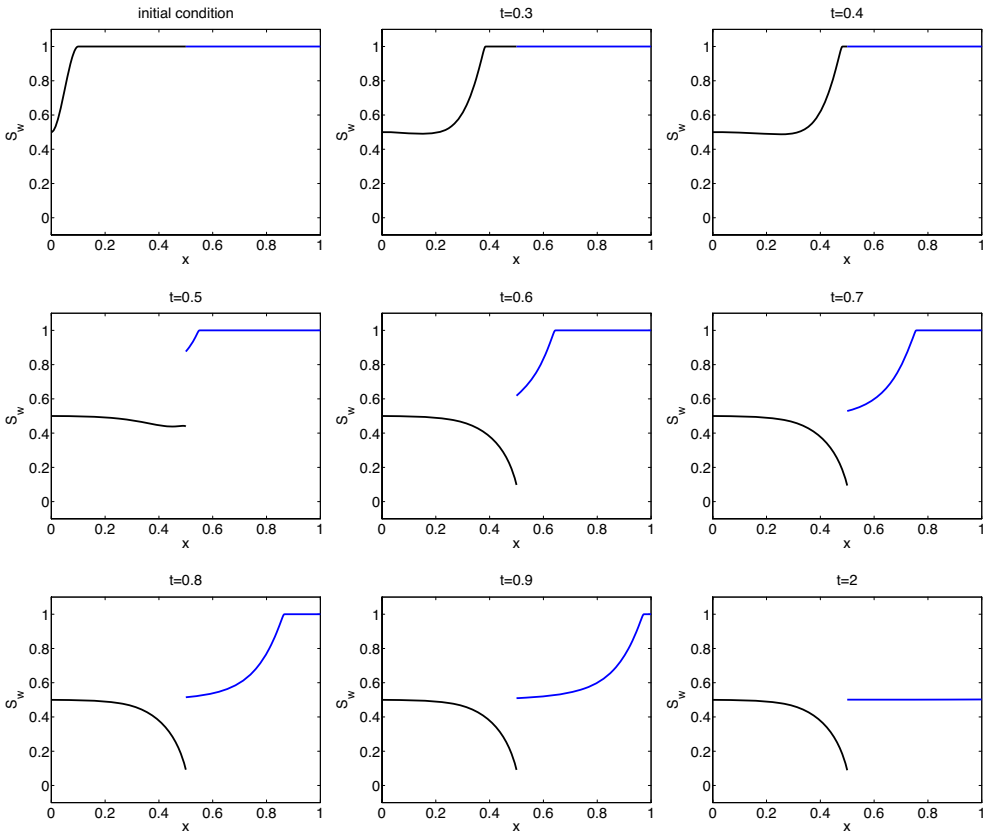

Fig. 11 $\tau_l = 0.05$, $\tau_r = 0.1$, solution at different timesteps

static capillary pressure is decreased. Comparing with the static case, see Fig. 3, we see a process that is locally nonreversible. This effect has also been observed in experiments [5, 6].

As time-asymptotic behavior, the saturation at the right side s^r converges to $s^{-\infty}$, and thus, $\frac{ds^r}{dt}$ converges to zero. Therefore, we see the same time-asymptotic limit as in the case of static capillary pressure. In particular, the two saturations at the right and left side are related by the same condition as in the static case.

3.3 Dynamic capillary-pressure – non-monotonous wave profile

For larger values of τ, a non-monotonous behavior of the saturation can occur at one or both sides of the interface. This implies that the dynamic term $\tau \frac{ds}{dt}$ can change the sign. Such a behavior can be interpreted as a sequence of local outflow and inflow processes with monotonous behavior, and thus, we see a dynamic capillary pressure that is enlarged while the saturation

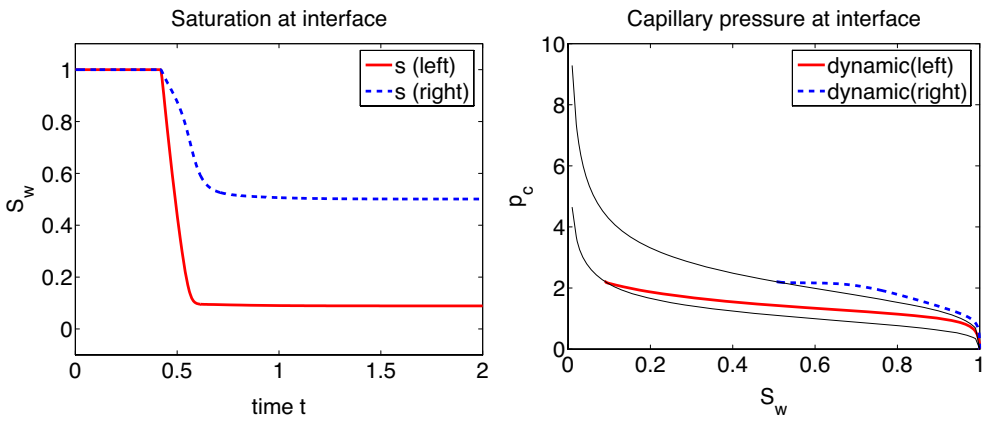

Fig. 12 $\tau_l = 0.05$, $\tau_r = 0.1$. *Left* behavior of the saturation at the interface, *right* static (reference) and dynamic capillary pressure

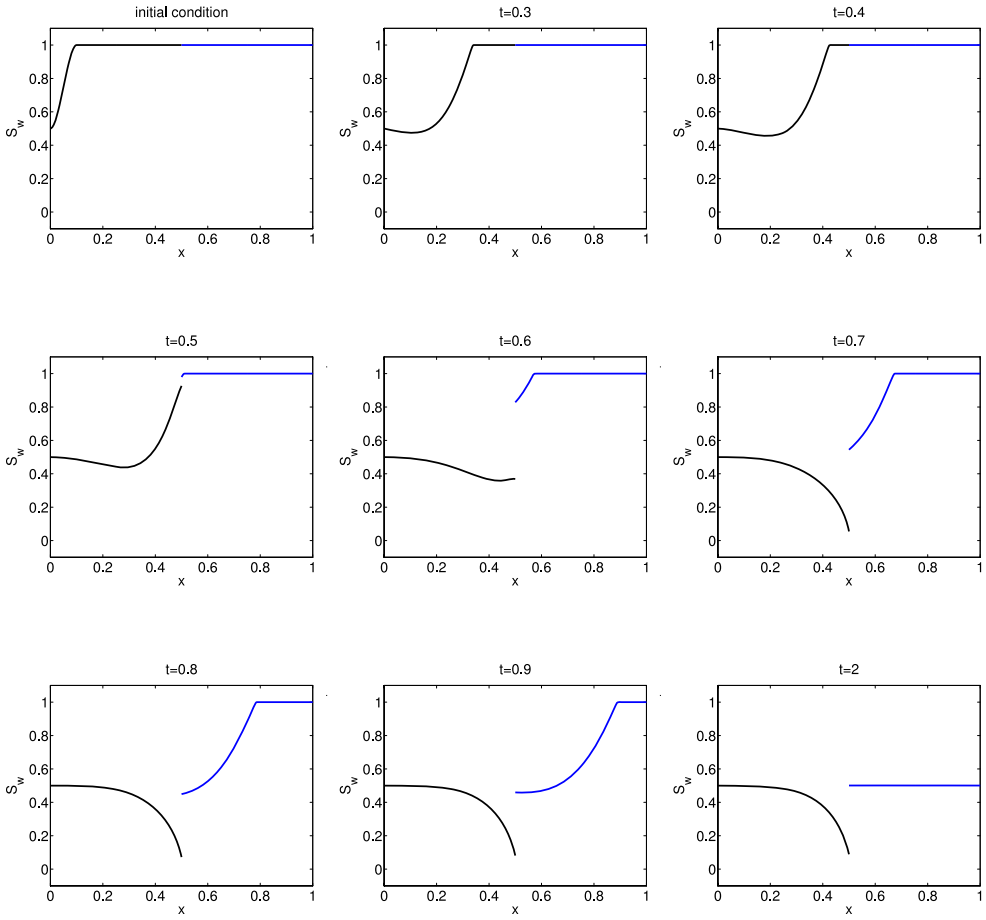

Fig. 13 $\tau_l = 0.1$, $\tau_r = 0.2$, solution at different timesteps

is decreasing, followed by a period where the capillary pressure is decreased while the saturation is increasing again, see Fig. 5. Therefore, one observes "loops" in the pressure–saturation graph, and thus, we have neither a unique relationship between capillary pressure and saturation nor vice versa.

4 Numerical model

In this section, we derive and describe the numerical model that is used in our simulations. We use a semi-implicit upwind finite volume scheme on each subdomain and deduce a suitable discretization for the

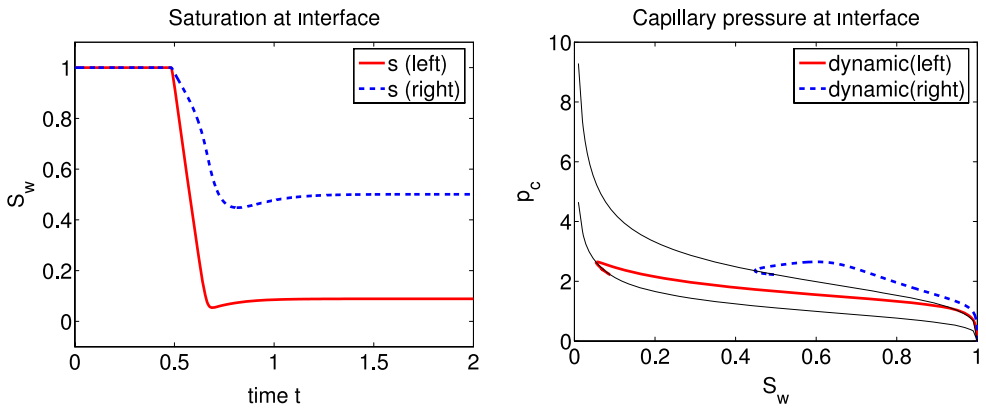

Fig. 14 $\tau_l = 0.1$, $\tau_r = 0.2$. *Left* behavior of the saturation at the interface, *right* static (reference) and dynamic capillary pressure

interface condition. The finite volume scheme is similar to the one proposed in [2].

4.1 Time-discretization

As time-discretization, we use the semi-implicit Euler scheme, i.e., an implicit Euler scheme where the nonlinearities are evaluated at the previous timestep. We introduce the timestep $t_{i+1} - t_i =: \Delta t$ and obtain for the time-approximation $s_i \approx s(t_i)$:

$$\phi \frac{s_{i+1} - s_i}{\Delta t} + \frac{d}{dx} F_i(s) = 0,$$

where $F_i(s)$ is the flux function,

$$F_i(s) := f_w(s_i) v_t + \bar{\lambda}(s_i) K \left(\left(\partial_s p_c^{\text{stat}} \right)(s_i) \partial_x s_{i+1} - \tau \frac{\partial_x s_{i+1} - \partial_x s_i}{\Delta t} \right).$$

We note that, for a linear capillary pressure relationship and no dynamic term, an explicit discretization in time shows good results. However, the dynamic capillary pressure implies an implicit discretization in time.

4.2 Space-discretization

For the spatial discretization, we use a finite volume scheme on a dual mesh and define suitable numerical flux functions. We only consider a finite interval of $\Omega = \mathbb{R}$. This interval is then split the computational subdomains Ω_l and Ω_r.

The computational domains Ω_k are divided into N_k intervals $[x^{n-1}, x^n]$ of length $\Delta x^n := x^n - x^{n-1}$. For simplicity of notation, we assume that, for each subdomain, all intervals are of the same length Δx_k. We define the midpoint of the intervals by $x^{n+1/2} := \frac{x^n + x^{n+1}}{2}$, $n = 0, \ldots, N-1$ and the dual mesh by the dual intervals $[x^{n-1/2}, x^{n+1/2}]$, see Fig. 6.

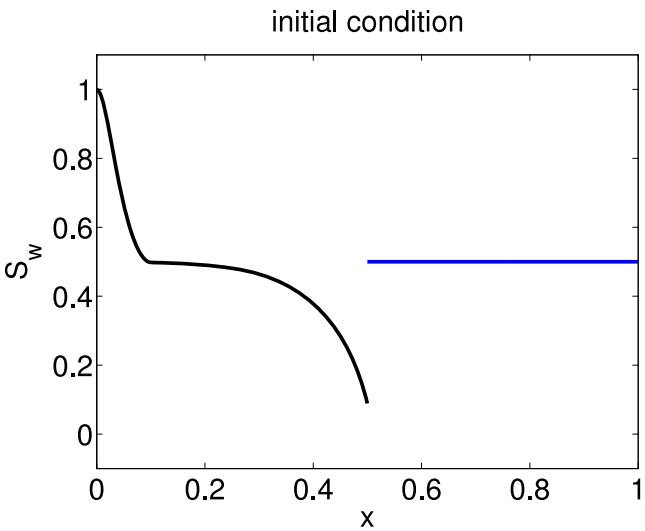

Fig. 15 Initial condition for inflow problem

Now, we use a finite volume scheme with the intervals of the dual mesh as integration domains. For equidistant intervals, the length of the inner intervals of the dual mesh is again Δx_k on each subdomain. The saturation s is then approximated by its mean value, $s^n = \frac{1}{\Delta x} \int_{x^{n-1/2}}^{x^{n+1/2}} s(x) dx$ and the fully discretized equation reads

$$\phi \frac{s_{i+1}^n - s_i^n}{\Delta t} + \frac{F_i(s^n, s^{n+1}) - F_i(s^{n-1}, s^n)}{\Delta x} = 0, \quad n = 1, \ldots, N,$$

where $F_i(s^n, s^{n+1})$ is the numerical flux defined by

$$F_i\left(s^n, s^{n+1}\right) := \alpha^{n+1/2} v_t + \beta^{n+1/2} \frac{s_{i+1}^{n+1} - s_{i+1}^n}{\Delta x} - \gamma^{n+1/2} \frac{s_{i+1}^{n+1} - s_{i+1}^n + s_i^{n+1} - s_i^n}{\Delta x \Delta t}.$$

The coefficients α, β, γ are defined in terms of s_i, the saturation at the previous timestep i, by:

$$\alpha^n := f_w\left(s_i^n\right), \ \beta^n := \bar{\lambda}\left(s_i^n\right) K \left(p_c^{\text{stat}}\right)'\left(s_i^n\right), \ \gamma^n := \bar{\lambda}\left(s_i^n\right) K \tau.$$

For β representing the diffusion term, a mean value is used. The terms α and γ are parts of the convective term. To get a stable numerical scheme, we therefore have to use upwinding on these terms. In our setting, we know that the total flux is constant and by assumption positive, we therefore set

$$\alpha^{n+1/2} := \alpha^n, \quad \beta^{n+1/2} := \frac{1}{2}\left(\beta^n + \beta^{n+1}\right), \quad \gamma^{n+1/2} := \gamma^n.$$

We note that, using this kind of semi-implicit time discretization, s_{i+1} can be computed by solving a linear system where the matrix entries and right hand side depend on s_i.

4.3 Discretization of the interface condition

We recall that, at the interface, discontinuities of the saturation can occur. This relationship between the saturation at both sides of the interface was specified by the interface condition (5). Moreover, the continuity of the flux through the interface was forced by the introduction of a Lagrange multiplier (4).

In our numerical model, we have to discretize the Lagrange multiplier in a suitable way. As we are in

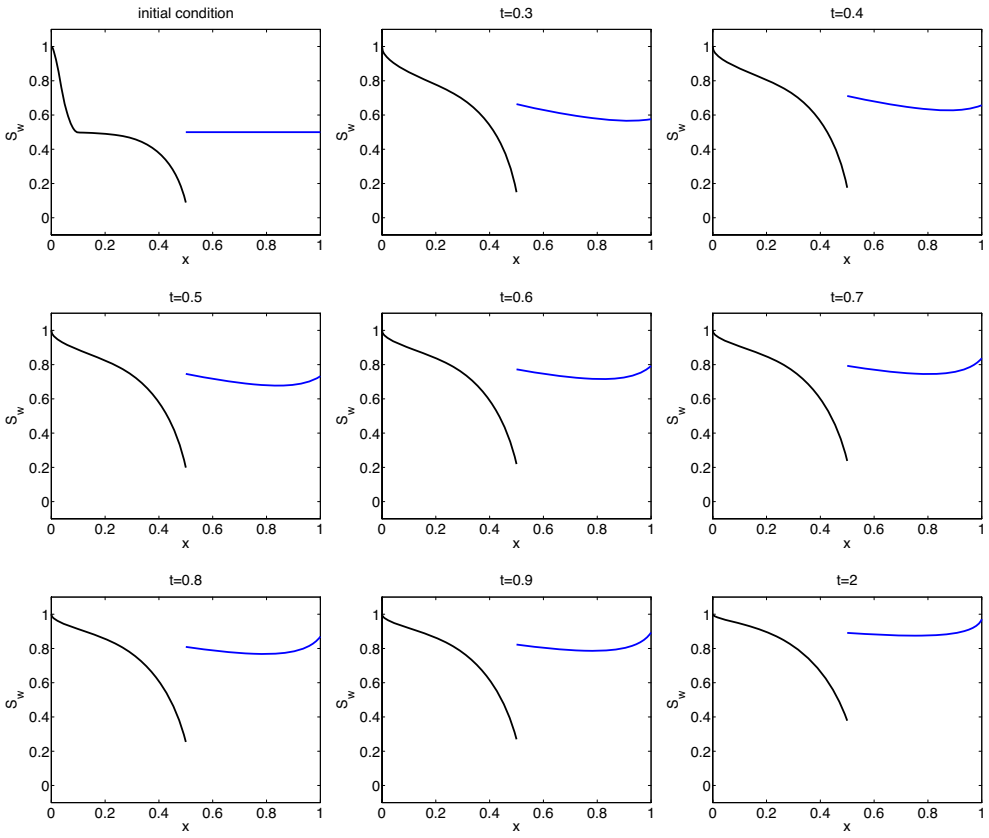

Fig. 16 $\tau_l = \tau_r = 0$, solution at different timesteps

the one-dimensional case, the flux through the interface yields just one new unknown $F_I \approx v_I$, see Fig. 7.

The interface condition (5) is discretized implicit in time,

$$p_{c,l}^{\text{stat}}\left(s_{i+1}^l\right) - \tau_l \frac{s_{i+1}^l - s_i^l}{\Delta t} = p_{c,r}^{\text{stat}}\left(s_{i+1}^r\right) - \tau_r \frac{s_{i+1}^r - s_i^r}{\Delta t}. \quad (8)$$

To get a linear equation for s_{i+1} also for the interface condition, the term $p_c^{\text{stat}}(s_{i+1})$ is approximated by

$$p_c^{\text{stat}}(s_{i+1}) \approx p_c^{\text{stat}}(s_i) + \left(p_c^{\text{stat}}\right)'(s_i)(s_{i+1} - s_i). \quad (9)$$

We note that, for a linear static capillary pressure–saturation relationship, the approximation is exact. Using (9) in (8) gives the linearized interface condition

$$p_{c,l}^{\text{stat}}\left(s_i^l\right) + \left(\left(p_{c,l}^{\text{stat}}\right)'\left(s_i^l\right) - \frac{\tau_l}{\Delta t}\right)\left(s_{i+1}^l - s_i^l\right) = p_{c,r}^{\text{stat}}\left(s_i^r\right) + \left(\left(p_{c,r}^{\text{stat}}\right)'\left(s_i^r\right) - \frac{\tau_r}{\Delta t}\right)\left(s_{i+1}^r - s_i^r\right). \quad (10)$$

We recall that the length of the control volume at the boundary of Ω_k is $\Delta x_k/2$. Then, using the linearized

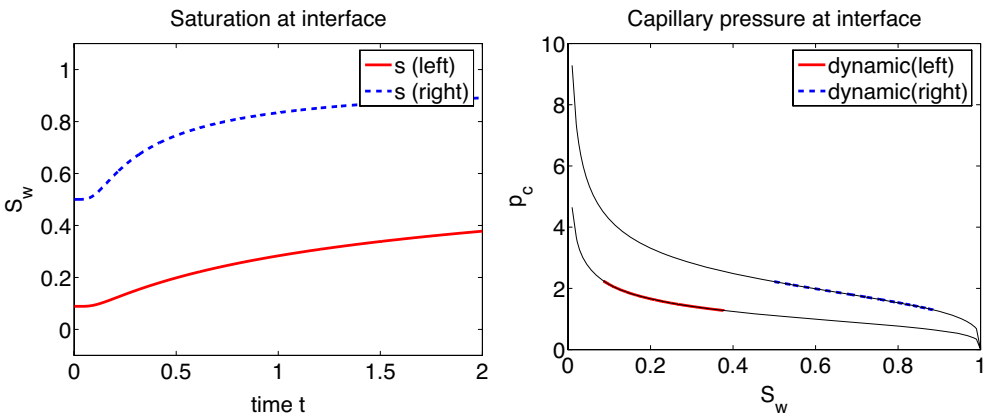

Fig. 17 $\tau_l = \tau_r = 0$, behavior at the interface

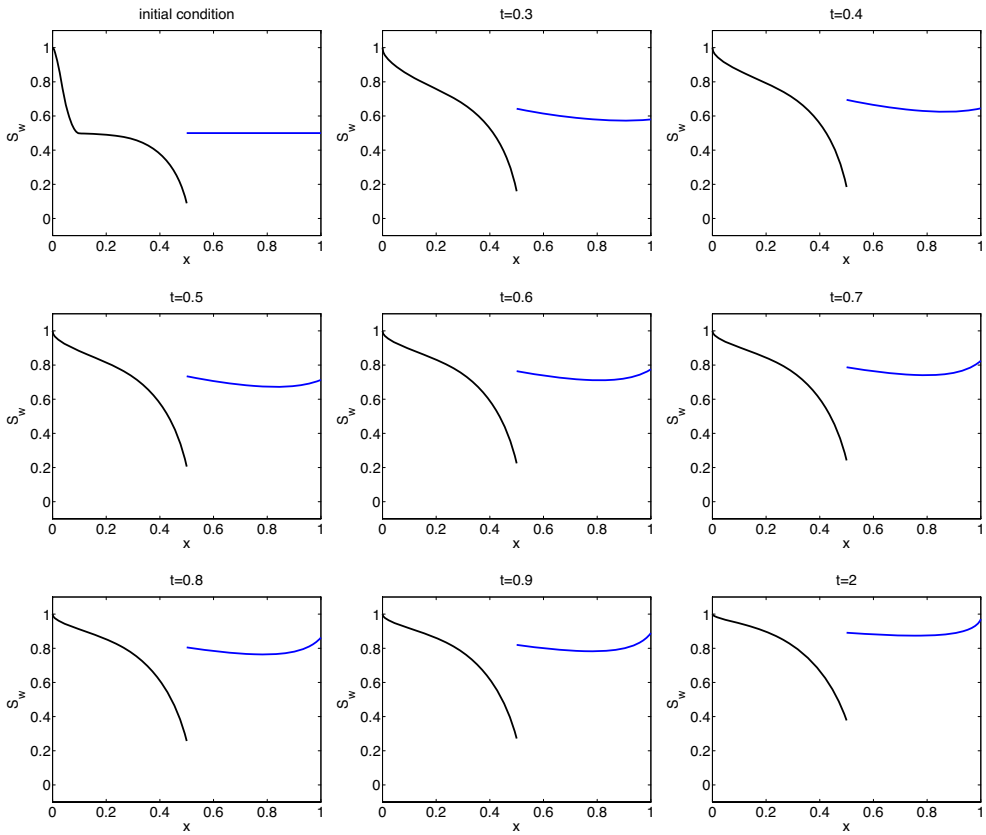

Fig. 18 $\tau_l = 0.1, \tau_r = 0.2$, solution at different timesteps

interface condition (10) and substituting on both subdomains, the flux through the interface by the Lagrange multiplier F_I, we get the following discrete equations, see Fig. 7,

$$\phi_l \frac{s_{i+1}^l - s_i^l}{\Delta t} + \frac{F_I - F^l(\ldots, s^l)}{\Delta x_l/2} = 0,$$

$$p_{c,l}^{\text{stat}} + \left(\left(p_{c,l}^{\text{stat}}\right)' - \frac{\tau_l}{\Delta t} \right) \left(s_{i+1}^l - s_i^l\right) = p_{c,r}^{\text{stat}} + \left(\left(p_{c,r}^{\text{stat}}\right)' - \frac{\tau_r}{\Delta t} \right) \times \left(s_{i+1}^r - s_i^r\right),$$

$$\phi_r \frac{s_{i+1}^r - s_i^r}{\Delta t} + \frac{F^r(s^r, \ldots) - F_I}{\Delta x_r/2} = 0.$$

5 Numerical simulation

5.1 Outflow problem

In our first three examples, we consider an outflow problem; that is, the water phase is displaced by the non-wetting phase. For simplicity, we assume $v_t = 1$, use $\phi_l = \phi_r = K_l = K_r = 1$, and a quadratic relative permeability function. Together with $\mu_\alpha = 1$, this leads to $\lambda_w(s) = s^2$, $\lambda_n(s) = (1-s)^2$.

We use $p_{c,l}^{\text{stat}}(s) = (s^{-4/3} - 1)^{1/4}$ and $p_{c,r}^{\text{stat}}(s) = 2(s^{-4/3} - 1)^{1/4}$, which corresponds to a van-Genuchten capillary

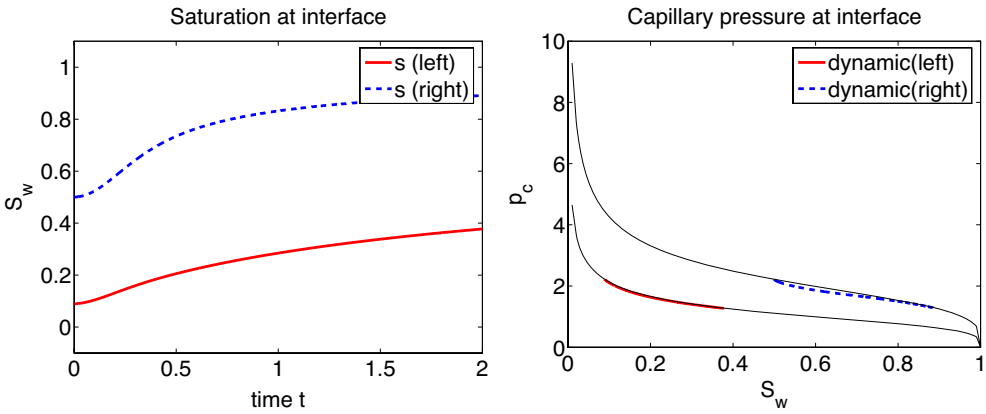

Fig. 19 $\tau_l = 0.1, \tau_r = 0.2$, behavior at the interface

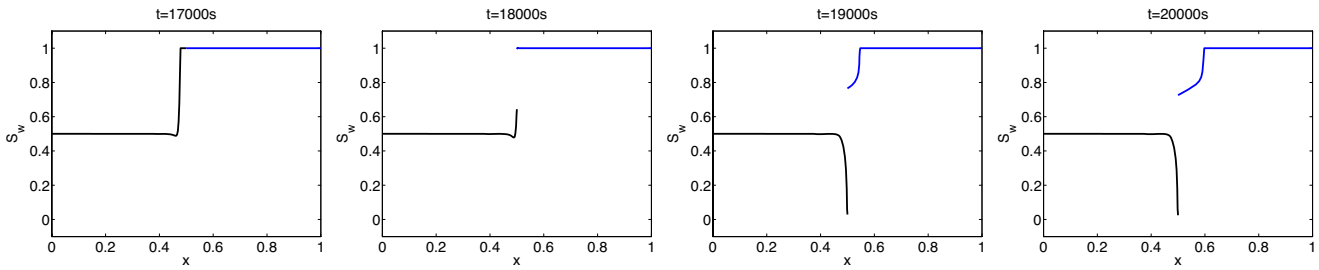

Fig. 20 Real-life example, solution at different timesteps

pressure relationship with $n = 4$, see [22]. The derivative of these function has a singularity at $s = 0$ and $s = 1$. Therefore, they are regularized in a small neighborhood of 0 and 1, respectively, and replaced by a linear function. We note that, in this model problem, the heterogeneity of the material is only modeled by the different capillary pressure functions on both subdomains.

The domain is given by $\Omega_l = (0, 0.5)$ and $\Omega_r = (0.5, 1)$. As initial condition, we use the cubic spline

$$s_0^{\text{out}}(x) = \begin{cases} -(x/10)^3 + 1.5(x/10)^2 + 0.5 & 0 < x < 0.1 \\ 1 & x \geq 0.1 \end{cases}. \quad (11)$$

The static capillary functions and the initial condition are depicted in Fig. 8. As boundary conditions, we impose a saturation of 0.5 at the left side of Ω_l and use absorbing (free flow) boundary conditions on the right side of Ω_r.

For the space discretization, we use a dual mesh with $\Delta x = 0.0025$ and a timestep of $\Delta t = 0.001$. We remark that the timestep has to be chosen small enough such that the Courant–Friedrich–Levy condition is fulfilled.

In the first example, we consider the problem with static capillary pressure relationship in both subdomains, i.e., $\tau_l = \tau_r = 0$. The solution at various timesteps is depicted in Fig. 9. We observe a wave with a monotone wave profile. On the left side of the interface, a pooling of the non-wetting phase can be determined. The solution in the given interval converges toward a static solution for the flow problem.

In Fig. 10, we can see the behavior at the interface. Due to the hyperbolic character of the problem, the same monotone behavior of the saturation with respect to time can be seen on both sides of the interface. On the right picture of Fig. 10, the static capillary pressure during the outflow process at both sides of the interface is plotted. As $\tau = 0$, the pressures exactly fit to the p_c function.

In the second example, we choose $\tau_l = 0.05$, $\tau_r = 0.1$. In this paper, a non-monotonous behavior of the wave profile can be observed in the domain Ω_l, see Fig. 11.

The behavior at the interface is quite similar to the first example, see Fig. 12. As the time derivate of s is negative, we observe an increased capillary pressure compared to the static capillary pressure relationship.

In the third example, we have $\tau_l = 0.1$, $\tau_r = 0.2$. The saturation for various timesteps is depicted in Fig. 13. For this values, we clearly see dynamic effects and observe non-monotonous wave profiles in both subdomains. At the interface, also a non-monotonous

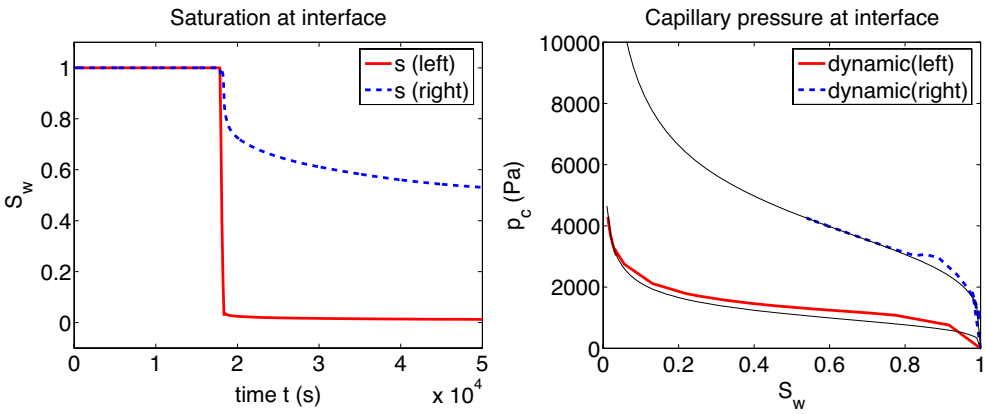

Fig. 21 Real-life example, behavior at the interface

behavior of the saturation can be observed, see Fig. 14. Therefore, some values of saturation are reached having a negative time derivative in the beginning and having a positive time derivative later. When considering the capillary pressure at the interface, this implies that the capillary pressure cannot be written as a well-defined function in terms of s, more precisely, some "loops" occur until the solution converges to a static solution.

5.2 Inflow problem

In our next examples, we consider an inflow problem. In this paper, the non-wetting phase is displaced by the water phase. We note that, at the interface, we start out of a static equilibrium condition satisfying the interface condition for a static problem. Moreover, on the left side, we want to use $s(0) = 1$ as boundary condition and a smooth transition. Denoting by s^{eq}, the equilibrium solution with $s(0) = 0.5$ and $s(1) = 0.5$ (which is the time-asymptotic limit for the outflow problem denoted above) and using the spline defined in (11), we use the following initial condition, see Fig. 15

$$s_0^{\text{in}} := \frac{s^{\text{eq}}}{s_0^{\text{out}}}.$$

We use the same material parameters and constitutive relationships as in the outflow problems, i.e., $\phi_l = \phi_r = K_l = K_r = 1$, $\lambda_w(s) = s^2$, $\lambda_n(s) = (1-s)^2$ and $p_{c,l}^{\text{stat}}(s) = (s^{-4/3} - 1)^{1/4}$, $p_{c,r}^{\text{stat}}(s) = 2(s^{-4/3} - 1)^{1/4}$ with the regularization introduced before. As time and space discretization, we use $\Delta x = 0.0025$ and $\Delta t = 0.001$ as in the previous examples.

The first example of inflow is with a static capillary pressure relationship, $\tau_l = \tau_r = 0$, see Fig. 16. The behavior at the interface can be seen in Fig. 17. As expected, we get the same relationships between the saturations and pressures as in the outflow problem, the only difference is the increasing saturation.

In the second inflow example, we use a dynamic capillary-pressure relationship with $\tau_l = 0.1$, $\tau_r = 0.2$. The solution at various timesteps is depicted in Fig. 18, and the behavior at the interface can be seen in Fig. 19. First of all, we see that, although a non-monotonous wave profile exists, we do not see a non-monotonous behavior at the interface. As a result, no loops are present in the capillary pressure picture, and we only see a small influence of the dynamic term.

Comparing this result with the outflow problems above, we see that the dynamic effect at the interface is less distinct for inflow problems.

5.3 Real-data application

We now apply our scheme to a dynamic outflow problem with realistic material parameters, see [15]. The domain Ω is given by $\Omega_l = (0m, 0.5m)$ and $\Omega_r = (0.5m, 1m)$. We assume flow from left to right with total velocity $v_t = 10^{-5} ms^{-1}$. The material parameters are given by $\phi_1 = \phi_2 = 0.4$ and $K_1 = 10^{-12} m^2$, $K_2 = 1.6 \cdot 10^{-11} m^2$. For the static capillary pressure in the left subdomain, we use a van-Genuchten relationship with $n = 4$ and $\alpha = 10^{-3} Pa^{-1}$,

$$p_{c,l}^{\text{stat}}(s) = 10^3 Pa \cdot (s^{-4/3} - 1)^{1/4}.$$

The Leverett relationship $p_c \sim \sqrt{\frac{\phi}{K}}$ (see [14]) then implies for the static capillary pressure in the right subdomain

$$p_{c,r}^{\text{stat}}(s) = 4 \cdot 10^3 Pa \cdot (s^{-4/3} - 1)^{1/4}.$$

As dynamic capillary factors, we choose $\tau_l = 10^5 Pas$ and $\tau_r = 4 \cdot 10^5 Pas$. For the fluids, we consider water with a viscosity of $\mu_w = 10^{-3} Pas$ and oil with viscosity $\mu_n = 10^{-3} Pas$. The relative permeability functions are given by $k_{rw} = s^2$ and $k_{rn} = (1-s)^2$. The initial and boundary conditions are chosen as in the model problem.

As discretization parameters, we use a meshsize of $\Delta x_l = 0.00125$ m and $\Delta x_r = 0.0025$ m and as time discretization $\Delta t = 50$ s.

The solution at some timesteps before and after the infiltration in the second subdomain is depicted in Fig. 20. Here we see, that the dynamic capillary term has a very small influence on the wave solution, only a small peak can be seen. However, because of the steep wave front, the behavior at the interface is nevertheless dominated by the capillary effect, see Fig. 21.

6 Final remarks

In this paper, we presented a new method to model and simulate two-phase flow in one-dimensional heterogeneous porous media under dynamic capillary conditions. Under the assumption of incompressible phases, the fractional flow formulation allowed us to separate the model into the pressure equation and the saturation equation. In this paper, the dynamic term in the capillary pressure–saturation relationship could be regarded as additional convective term. The key point to model the process at material discontinuities was using a Lagrange multiplier, which represents the flux at the material interface. The model was discretized in

a natural way, and thus, the numerical model yields the flux through the interface as additional unknown. In our numerical simulations, we applied the method to outflow and inflow problems. For a small dynamic influence, the shape of the traveling wave did not change much compared to the non-dynamic case. However, the influence of the dynamic capillary pressure at the material interface could be clearly observed.

For two- and three-dimensional problems, the idea of using a Lagrange multiplier representing the flux and an interface condition can be directly transferred. In this paper, only the fluxes normal to the interface have an influence in the modeling of saturation relationships. Then, this flux plays the role of the dual variable in a mortar setting. Therefore, special care has to be taken in the space discretization: The discrete flux has to be chosen in a suitable space with respect to the discretization of the saturation such that the solvability and optimality can be guaranteed. This will be considered in a forthcoming paper.

Acknowledgements This work was supported by the Deutsche Forschungsgemeinschaft (German Research Foundation), SFB404. We thank Helge Dahle and Sabine Manthey for their useful help and fruitful discussions.

References

1. Charbeneau, R.: Groundwater Hydraulics and Pollution Transport. Prentice Hall, Upper Saddle River (2000)
2. Cuesta, C.: Pseudo-parabolic equations with driving convection term. Ph.D. thesis, VU Amsterdam, Netherlands (2003)
3. Cuesta, C., Duijn, C.V., Hulshof, J.: Infiltration in porous media with dynamic capillary pressure: Travelling waves. Euro. J. Appl. Math **11**, 381–397 (2000)
4. de Neef, M.: Modelling capillary effects in heterogeneous porous media. Ph.D. thesis, University of Delft, The Netherlands (2000)
5. DiCarlo, D.: Experimental measurements of saturation overshoot on infiltration. Water Resour. Res. **40**, W04215 (2004)
6. DiCarlo, D.: Modeling observed saturation overshoot with continuum additions to standard unsaturated theory. Adv. Water Resour. **40**, 1021–1027 (2004)
7. Hassanizadeh, S., Celia, M., Dahle, H.: Experimental measurements of saturation overshoot on filtration. Vadose Zone J. **1**, 38–57 (2002)
8. Hassanizadeh, S., Gray, W.G.: Mechanics and thermodynamics of multi-phase flow in porous media including interphase boundaries. Adv. Water Res. **13**(4), 169–186 (1990)
9. Hassanizadeh, S., Gray, W.G.: Thermodynamic basis of capillary pressure on porous media. Water Resour. Res. **29**(10), 3389–3405 (1993)
10. Hassanizadeh, S., Oung, O., Manthey, S.: Laboratory experiments and simulations on the significance on non-equilibrium effect in capillary pressure-saturation relationship. In: Unsaturated Soils: Experimental Studies, Proceedings of the International Conference from Experimental Evidence Towards Numerical Models in Unsaturated Soils. Weimar 2005, vol. 93, pp. 3–14 Springer Proceedings in Physics. Springer (2005)
11. Helmig, R.: Multiphase Flow and Transport Processes in the Subsurface. Springer (1997)
12. Helmig, R., Huber, R.: Comparison of Galerkin-type discretization techniques for two-phase flow in heterogeneous porous media. Adv. Water Res. **21**, 697–711 (1998)
13. LeFloch, P.: Hyperbolic Systems of Conservation Laws: The Theory of Classical and Nonclassical Shock Waves. Birkhäuser (2002)
14. Leverett, M.C.: Capillary behavior in porous soils. Trans. AIME **142**, 152–169 (1941)
15. Manthey, S.: Two-phase processes with dynamic effects in porous media – parameter estimation and simulation. Ph.D. thesis, Institut für Wasserbau. Universität Stuttgart, Germany (2006)
16. Middendorf, J.: Zur Beschreibung des kapillaren Flüssigkeitstransports. Paper. Ph.D. thesis, Fakultät für Maschinenbau und Verfahrenstechnik, Technische Universität Chemnitz, Germany (2000)
17. Nieber, J., Dautov, R., Egorov, A.: Dynamic capillary pressure mechanism for instability in gravity-driven flows: Review and extension to very dry conditions. In: Das, D.B., Hassanizadeh, S.M. (eds.) Upscaling Multiphase Flow in Porous Media, pp. 147–172. Springer (2005)
18. Niessner, J., Helmig, R., Jakobs, H., Roberts, J.: Interface conditions and linearization schemes in the Newton iterations for two-phase flow in heterogeneous porous media. Adv. Water Res. **28**, 671–687 (2005)
19. van Duijn, C., Molenaar, J., de Neef, M.: Effects of capillary forces on immiscible two phase flow in heterogeneous porous media. Transp. Porous Media **21**, S. 71–93 (1995)
20. van Duijn, C., Peletier, L.: Nonstationary filtration in partially saturated porous media. Archs. Rat. Mech. Anal. **78**, 173–198 (1982)
21. van Duijn, C., Peletier, L., Pop, I.: A New Class of Entropy Solutions of the Buckley–Leverett Equation. Stichting Centrum voor Wiskunde en Informatica, Amsterdam (2005)
22. van Genuchten, M.: A close-form equation for predicting the hydraulic conductivity of unsaturated soils. Soil Sci. Soc. Am. J. **44**, 892–898 (1980)